

Supplementary Material

Exploring Uncharted Multiband Hyperbolic Dispersion in Conjugated Polymers: A First-Principles Study

Suim Lim^{1,2}, Dong Hee Park³, Bin Chan Joo³, Yeon Ui Lee^{3,*}, Kanghoon Yim^{1,*}

¹Energy AI & Computational Science Laboratory, Korea Institute of Energy Research, Gajeong-ro 152, Daejeon, 34129, Republic of Korea

²Department of Mechanical Engineering, Sogang University, Baekbeom-ro 35, Seoul, 04107, Republic of Korea

³Department of Physics, Chungbuk National University, Chungdae-ro 1, Cheongju, Chungbuk 28644, Republic of Korea

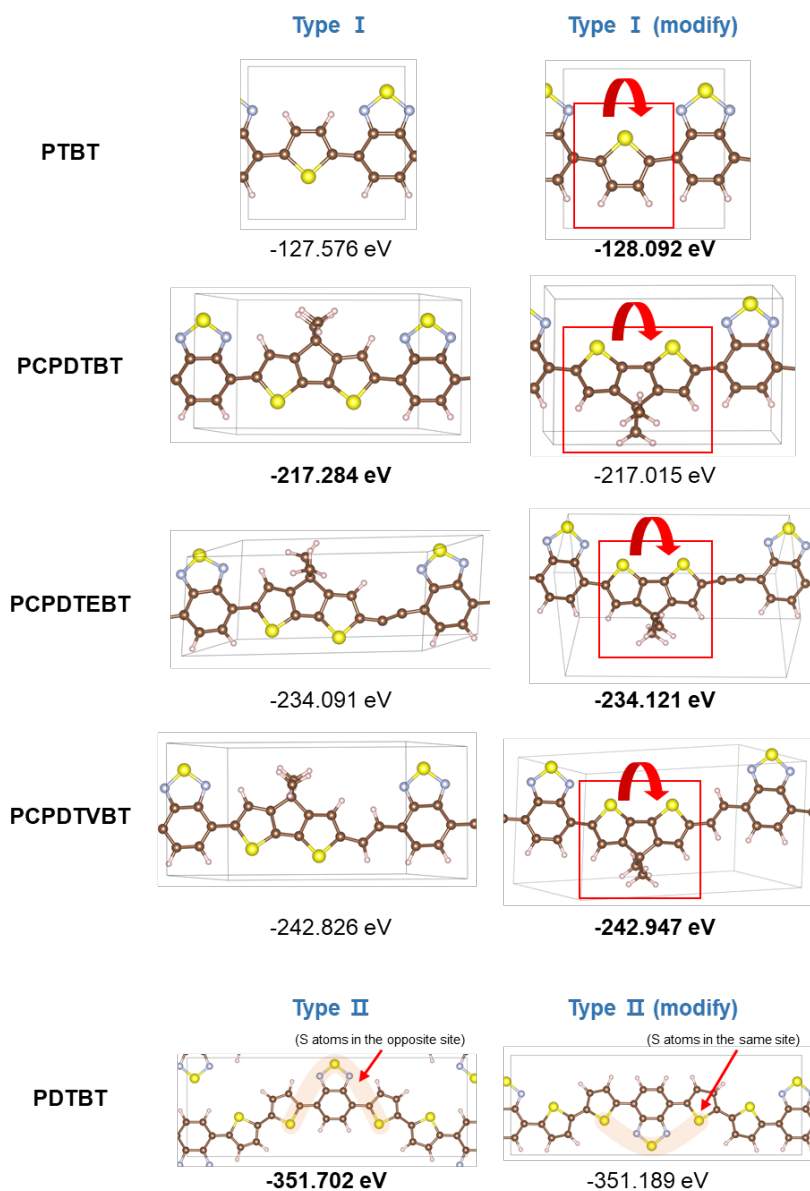
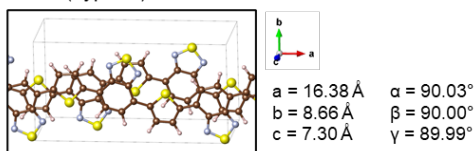


Fig. S1 The calculated total energies of the target polymers, accounting for the possible directional arrangements of assembly units within the Type I unit-cell. For PDTBT, the Type II unit cell is used for comparison, as the modified Type I unit-cell shares the same symmetry as the original.

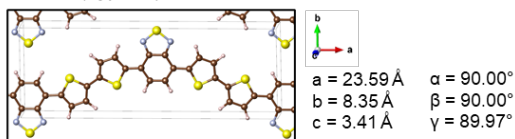
Table S1. Calculated polymerization energies (ΔE_{poly}) of various types for each copolymer.

	ΔE_{poly} (eV)			
	Type I	Type II	Type III	Type IV
PTBT	-1.182	-1.880	-1.213	-2.032
PDTBT	-2.055	-2.206	-2.085	-2.009
PCPDTBT	-1.836	-2.043	-1.864	-2.010
PCPDTEBT	-2.281	-1.968	-2.364	-1.971
PCPDTVBT	-2.253	-1.902	-2.366	-2.090

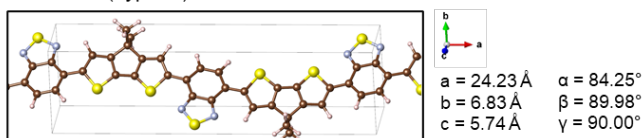
PTBT (Type IV)



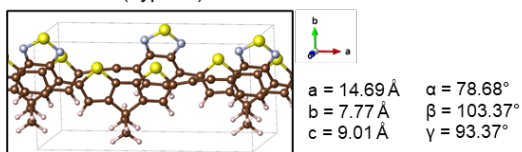
PDTBT (Type II)



PCPDTBT (Type II)



PCPDTEBT (Type III)



PCPDTVBT (Type III)

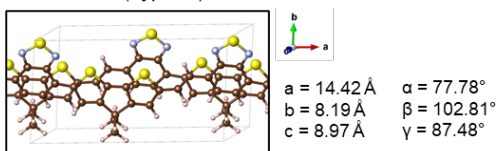


Fig. S2 The most stable structures of target copolymers that are searched among the four conformation types (Type I - IV as shown in **Fig. 1(b)**).

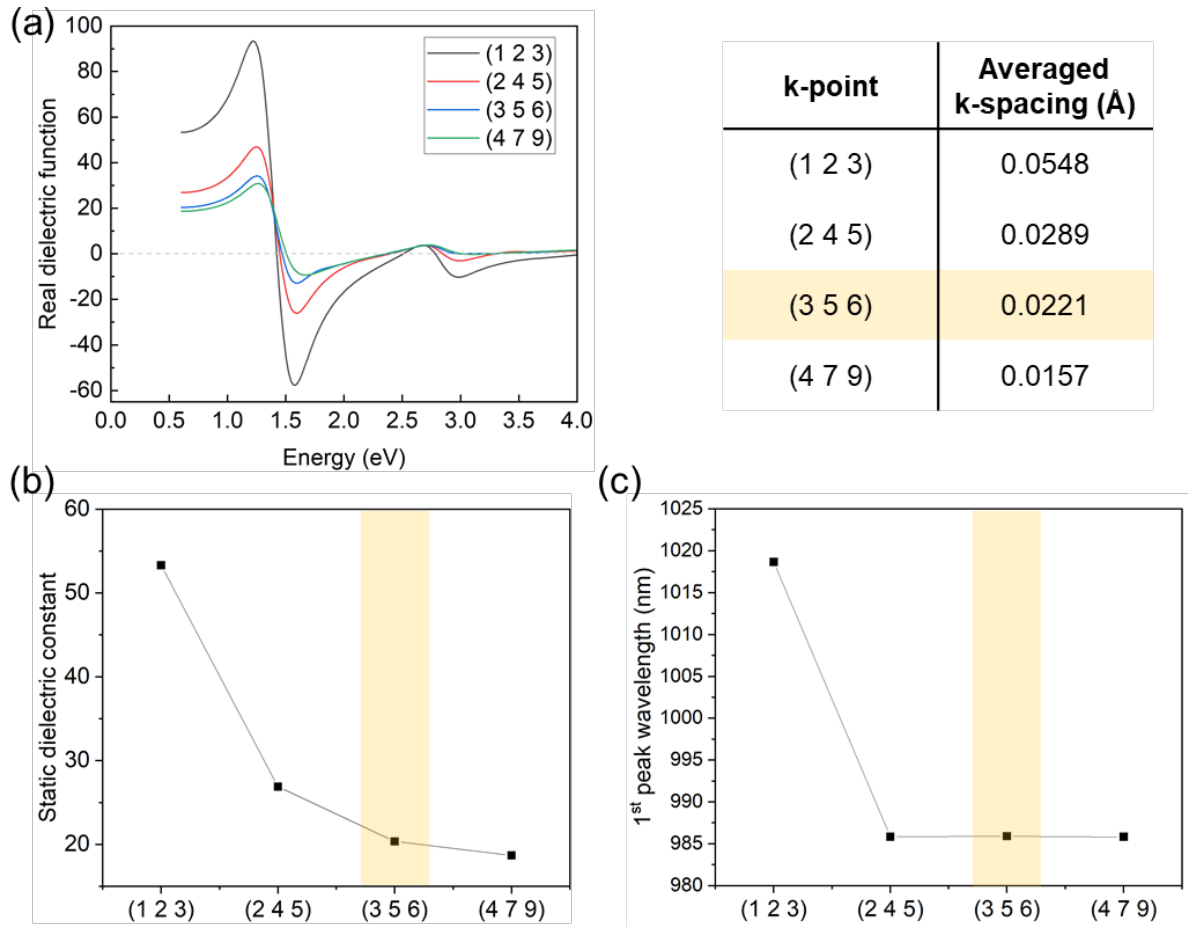
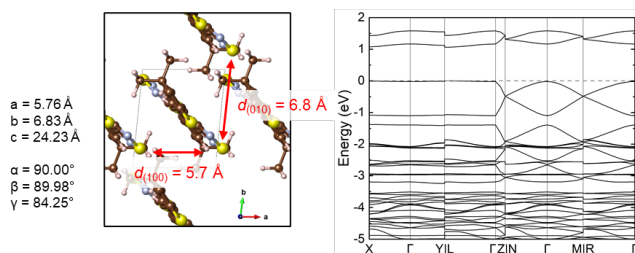


Fig. S3 The convergence test of a \mathbf{k} -spacing for the PTBT crystal structure is presented as an example. (a) Real dielectric function of PTBT with various \mathbf{k} -points. The convergence test results are shown for (b) the static dielectric constant and (c) the wavelength of the first peak in the dielectric function. A \mathbf{k} -spacing of 0.02 \AA^{-1} (yellow highlights) shows good convergence in both the static dielectric constant and the first peak in the dielectric function.

w/o vdW correction



w/ vdW correction

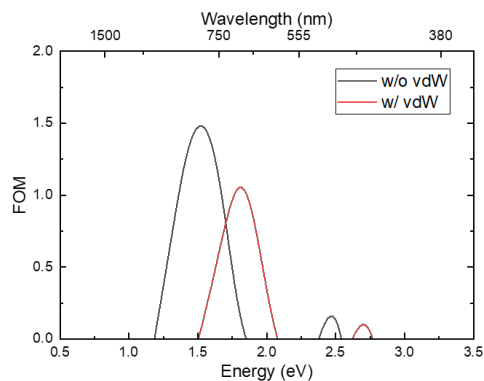
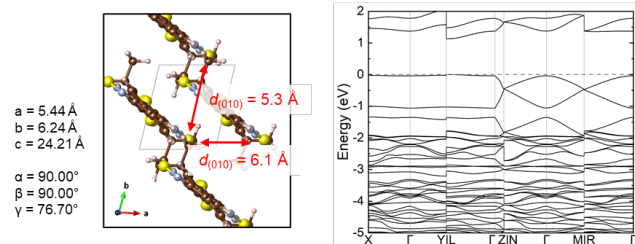


Fig. S4 The impact of the van der Waals (vdW) approximation using the Grimme-D3 method⁴⁹ on the lattice parameters, band structures, and FoM of PCPDTBT. The calculated FoM indicates that the volume changes resulting from vdW corrections primarily influence the spectral range of HD, while the multiband HD properties remain preserved.

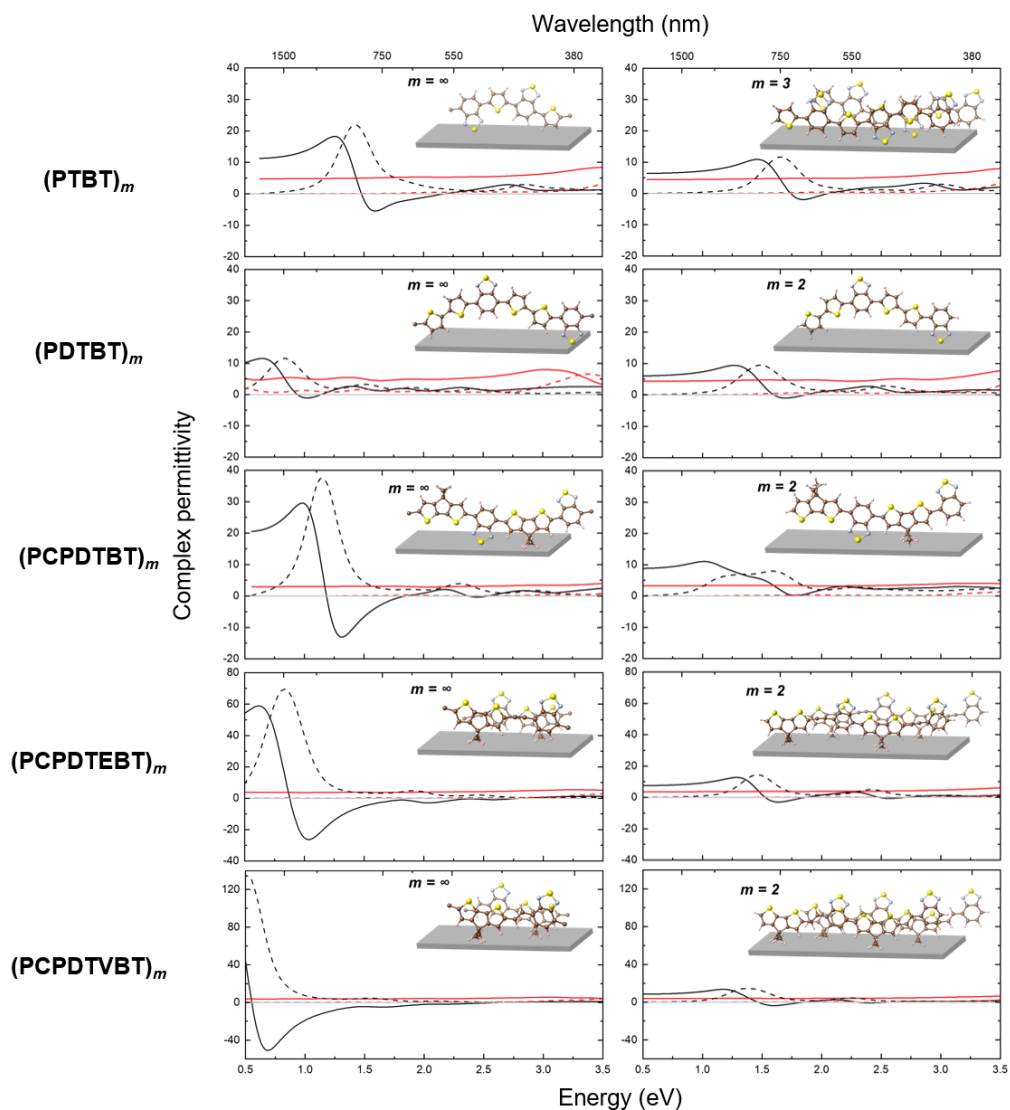


Fig. S5 Calculated complex permittivity of all considered copolymers. The graphs of crystalline polymer structures ($m = \infty$) are shown on the left, and those of the oligomer structures with specific m are shown on the right. The $\text{Re}(\epsilon)$ and $\text{Im}(\epsilon)$ are presented with solid lines and dashed lines, respectively. The red and black lines represent the H -direction and Z -direction, respectively.

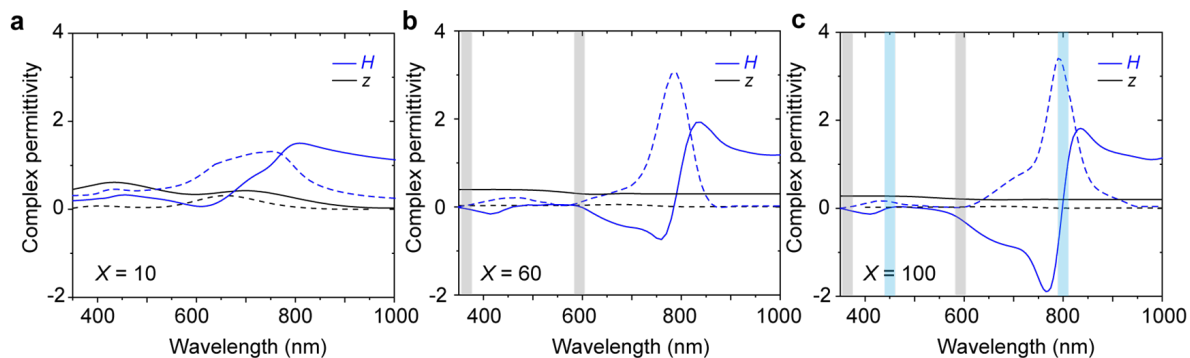


Fig. S6 The measured complex permittivity spectra of PCPDTBT films prepared from solutions containing $X = 10$, 60, and 100 mg of PCPDTBT in 1 ml of chlorobenzene (CB): (a) $X = 10$ mg/ml, (b) $X = 60$ mg/ml, and (c) $X = 100$ mg/ml.

PCPDTBT (Sigma-Aldrich, average Mw 14,000 g/mol) solutions were prepared by dissolving $X = 10$, 60, and 100 mg portions of PCPDTBT in 1 ml of chlorobenzene (CB). The solutions were heated at 50°C for 3 hours and spin-coated onto cleaned glass substrates to form thin polymer films. The films were spun at 2000 rpm for 500 seconds, followed by an additional 10 seconds at 5000 rpm. The resulting film thicknesses were measured as 72 nm, 127 nm, and 147 nm, respectively, using variable angle spectroscopic ellipsometry (VASE). Additionally, VASE was used to measure the complex permittivity spectra of the films (**Fig. S5**). The spectra for each concentration are shown: (a) 10 mg/ml, (b) 60 mg/ml, and (c) 100 mg/ml. The PCPDTBT films prepared from $X = 60$ mg/ml and $X = 100$ mg/ml solutions exhibit dual-band hyperbolic dispersion characteristics, as predicted by first-principles calculations.

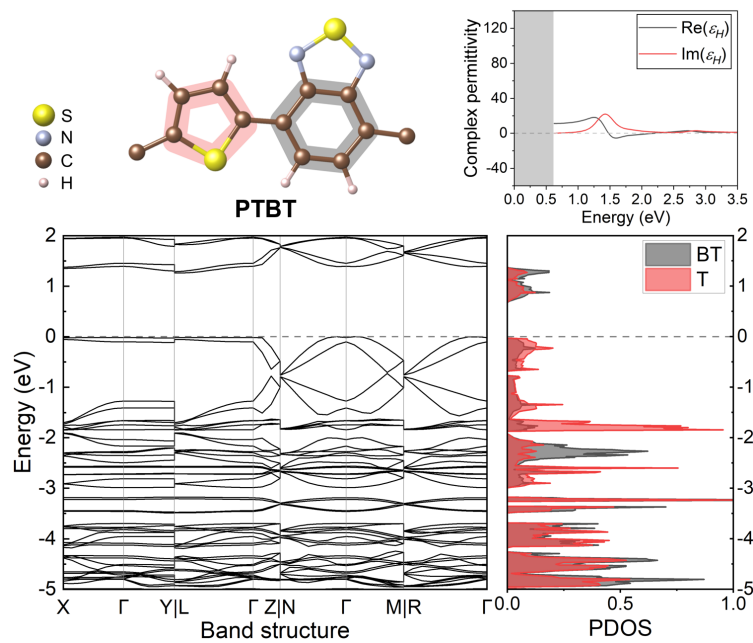


Fig. S7 The detailed analysis of PTBT with the calculated band structure, partial-density-of-state (PDOS) for carbon, and complex permittivity. PTBT has a gap of 1.26 eV.

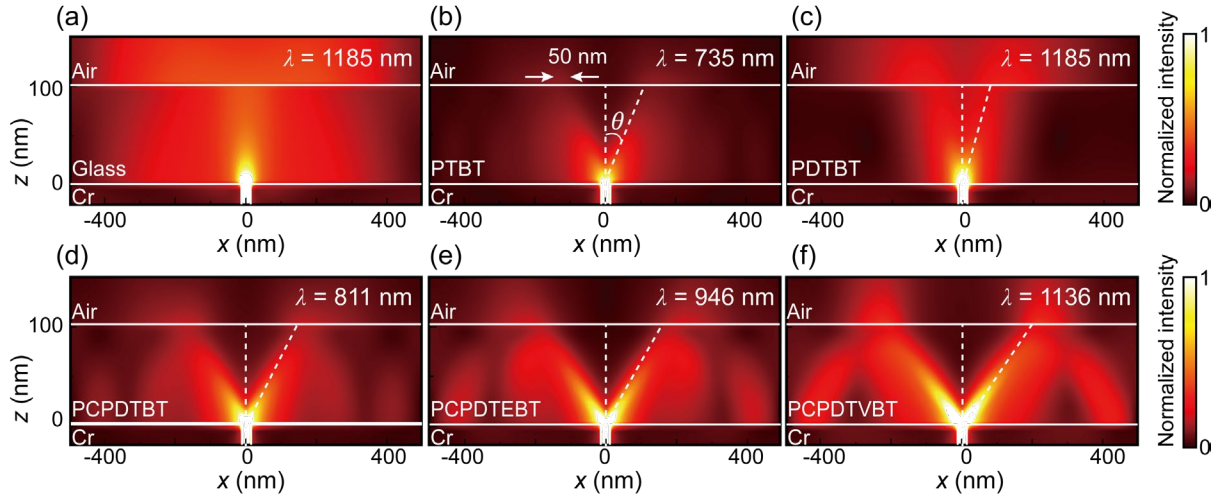


Fig. S8 FDTD simulation of light propagation in (a) glass and (b-f) conjugated polymers at the wavelength with the highest FOM. Glass does not propagate high- k modes well over long distances. On the other hand, OHMs can propagate high- k modes, achieving subwavelength light confinement due to their HD optical properties.

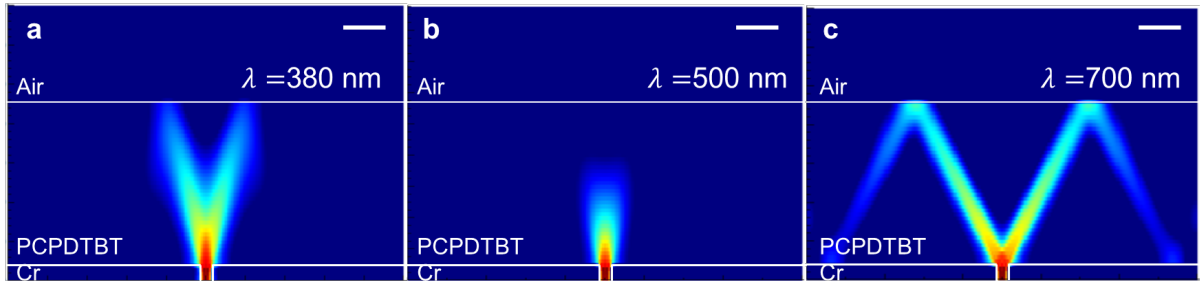


Fig. S9 FDTD simulations of light propagation in the PCPDTBT film at (a) $\lambda = 380$ nm, (b) $\lambda = 500$ nm, and (c) $\lambda = 700$ nm. The measured complex permittivity of the PCPDTBT film was used for these calculations. Scale bar: 100 nm.

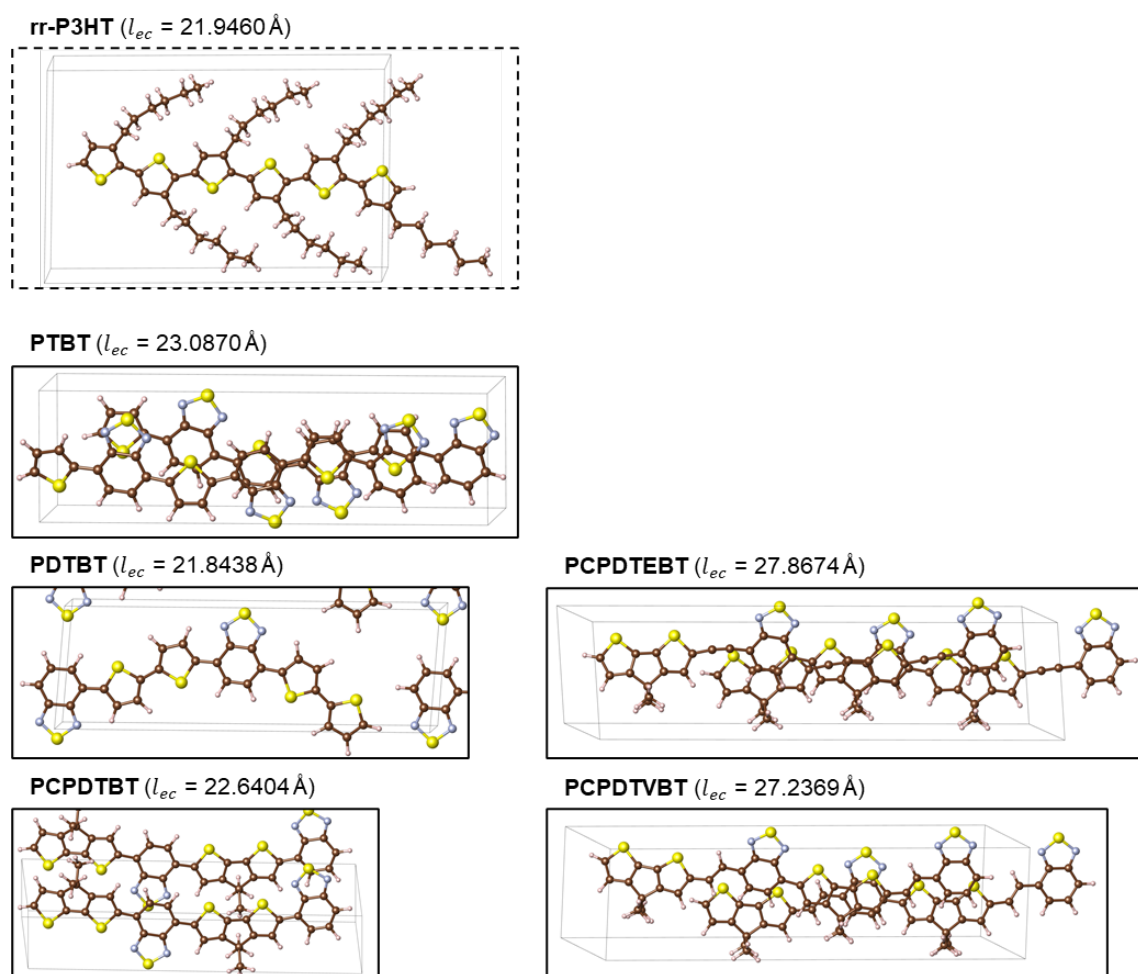


Fig. S10 Oligomer structures of each conjugated polymer with effective conjugation length (l_{ec}). The effective conjugation lengths are determined to be as close as possible to that of rr-P3HT¹⁶.

S11. Advantages of proposed OHMs in fabrication over conventional dielectric-metal multilayer HMMs

Unlike the multistep deposition process required for dielectric-metal multilayer HMMs, which demands precise control over layer thickness and interface quality, OHMs are fabricated using a simpler solution-based spin-coating method. This approach streamlines the fabrication process while minimizing interfacial imperfections, a major source of optical losses in traditional HMMs.

The solution-processing method enables uniform film deposition with tunable thickness and crystalline properties, eliminating the need for nanoscale precision in multilayer structures. This is particularly advantageous for maintaining hyperbolic dispersion, which is challenging in conventional HMMs.

Additionally, OHMs are compatible with large-scale, flexible, and lightweight substrates, making them ideal for applications such as flexible or wearable devices. In contrast, traditional HMMs are constrained by their rigid and brittle nature.

The organic nature of OHMs, coupled with their solution-based fabrication process, not only reduces material and processing costs but also lessens environmental impact compared to vacuum-based deposition methods used for conventional HMMs. These features collectively position OHMs as a superior alternative for advanced optical applications.